Recep Tayyip Erdoğan Üniversitesi Fen ve Mühendislik Bilimleri Dergisi, 7 (1) 262-274 2026
Recep Tayyip Erdogan University Journal of Science and Engineering, 7 (1) 262-274 2026
ISSN: 2687-2315 / E-ISSN: 2757-7686

Coupled-Channel Analysis of Heavy Ion Fusion Reactions and Barrier Distributions

Burcu EROL *

* Department of Physics, Faculty of Arts and Sciences, Recep Tayyip Erdoğan University, 53100, Rize, Türkiye

Sorumlu Yazar/Corresponding Author
E-mail: burcu.karayunus@erdogan.edu.tr

Araştırma Makalesi/Research Article
Geliş Tarihi/Received: 26.11.2025
Kabul Tarihi/Accepted: 24.03.2026

Abstract

This study presents a systematic investigation of the fusion dynamics for several heavy-ion systems (^{30}Si+ ^{26}Mg, ^{32}S+ ^{58}Ni, ^{46,48,50}Ti+ ^{124}Sn,^{58}Ni+ ^{58,64}Ni, ^{64}Ni+^{64}Ni, ^{64,70}Zn+ ^{64,70}Zn) near and below the Coulomb barrier. The effects of low-energy 2^+ and 3^- vibrational and rotational states on fusion cross-sections and barrier distributions were evaluated using the Coupled-Channels (CC) theoretical framework. A comparative analysis between different numerical implementations (CCFULL and NRV) and the one-dimensional barrier penetration model (Wong approximation) is performed to identify the sensitivity of sub-barrier fusion enhancement to specific channel couplings. The results demonstrate that while the CC approach generally provides a robust description of the experimental data, systematic discrepancies emerge in asymmetric systems and deep sub-barrier regimes, highlighting the limitations of simplified coupling schemes. This work provides a benchmark for code reliability and discusses the physical origins of model-dependent variations in predicting fusion probabilities for medium-mass nuclei.

Keywords: Heavy-ion, fusion, cross section, barrier distribution.

Ağır İyon Füzyon Reaksiyonları ve Bariyer Dağılımlarının Çiftlenmiş Kanal Analizi

Öz

Bu çalışma, Coulomb bariyeri civarında ve altındaki çeşitli ağır iyon sistemlerinin (^{30}Si+ ^{26}Mg, ^{32}S+ ^{58}Ni, ^{46,48,50}Ti+ ^{124}Sn,^{58}Ni+ ^{58,64}Ni, ^{64}Ni+^{64}Ni, ^{64,70}Zn+ ^{64,70}Zn) füzyon dinamiklerini sistematik olarak incelemektedir. Kanallara Bağlı (Coupled-Channels - CC) kuramsal çerçeve kullanılarak, düşük enerjili 2^+ ve 3^- titreşimsel ve dönme durumlarının füzyon tesir kesitleri ve bariyer dağılımları üzerindeki etkileri değerlendirilmiştir. Farklı sayısal uygulamalar (CCFULL ve NRV) ile tek boyutlu bariyer nüfuz modeli (Wong yaklaşımı) arasında karşılaştırmalı bir analiz yapılarak, bariyer altı füzyon artışının belirli kanal eşleşmelerine olan duyarlılığı belirlenmiştir. Sonuçlar, CC yaklaşımının deneysel verileri genel olarak tutarlı bir şekilde açıkladığını, ancak asimetrik sistemlerde ve bariyerin çok altındaki (deep sub-barrier) bölgelerde ortaya çıkan sistematik sapmaların, basitleştirilmiş eşleşme şemalarının sınırlılıklarını ortaya koyduğunu göstermektedir. Bu çalışma, kullanılan kodların güvenilirliği için bir kıyaslama sunmakta ve orta kütleli çekirdeklerin füzyon olasılıklarının tahmin edilmesindeki model kaynaklı varyasyonların fiziksel kökenlerini tartışmaktadır.

Anahtar kelimeler: Ağır iyon, füzyon, tesir kesiti, bariyer dağılımı.

Cite as;
Erol, B. (2026). Coupled-Channel Analysis of Heavy Ion Fusion Reactions and Barrier Distributions. *Recep Tayyip Erdogan University Journal of Science and Engineering*, 7(1), 262-274. Doi: 10.53501/rteufemud.1830481

1. Introduction

The interactions of heavy ions at low energies, particularly fusion processes occurring near and below the Coulomb barrier, have received extensive attention in the nuclear physics literature, both in terms of theoretical modeling and experimental observations (Montagnoli and Stefanini, 2023; Del Fabbro et al., 2023; Denisov, 2023). Reactions occurring in these energy ranges are crucial not only for understanding astrophysical processes such as the chemical evolution of the universe and energy production within stars, but also for understanding the nature of interactions at the nuclear level (Singh et al., 2021; Deng et al., 2025).

The fusion of two low-energy atomic nuclei to form a larger nucleus is made possible by quantum tunneling, a phenomenon that offers important insights into both the structure of energy barriers and the dynamic behavior of interacting nuclei (Jiang et al., 2023; Denisov and Jin, 2022; Cheng et al., 2022). In this context, the theoretical framework is based on modeling the total potential energy acting between the nuclei, composed of the long-range repulsive Coulomb contribution, the centrifugal term, and the short-range attractive nuclear force. The combination of these contributions defines the fusion barrier that must be surpassed for fusion to occur. When the relative kinetic energy of the colliding nuclei is insufficient to surpass this barrier classically, quantum tunneling enables sub-barrier penetration, leading to the formation of a compound nucleus (Montagnoli and Stefanini, 2023; Denisov, 2023).

Extensive theoretical and experimental studies have shown that the observed significant increase in fusion cross-section is generally accepted to be due to channel-coupling effects, which arise from the interaction of the relative motions of the colliding nuclei with the other degrees of freedom (Vijay et al., 2022). Therefore, the primary objective of the present study is to investigate the physical limits and the origins of discrepancies in the performance of various coupled-channel computation codes, such as CCFULL, CCFUS, CCDEF, and NRV (Fernández Niello et al., 1989; Hagino et al., 1999; Dasso, 1987; NRV Web Knowledge Base, 2020). In this study, fusion excitation functions for ^{30}Si+ ^{26}Mg, ^{32}S+ ^{58}Ni, ^{46,48,50}Ti+ ^{124}Sn,^{58,64}Ni+ ^{58,64}Ni, ^{64,70}Zn+ ^{64,70}Zn heavy-ion systems were calculated within the framework of the one-dimensional barrier transition model (1D-BPM) and the coupled-channels model. The scattering potential was considered as the sum of the Coulomb potential and the proximity potential (Erol et al., 2021; Gharaei et al., 2021). The theoretical findings were evaluated through a comparative analysis with experimental data to identify how different implementations of coupling affect the results. Furthermore, reduced reaction cross sections were evaluated, and the physical reasons behind the agreement or divergence between theoretical modeling and experimental observations were discussed in detail.

2. Theoretical Framework

The theoretical description of low-energy heavy-ion fusion requires a robust treatment of the coupling between the relative motion of the colliding nuclei and their internal degrees of freedom. In this work, the Coupled-Channels formalism is employed as the primary investigative tool, while the 1D-BPM (One-Dimensional Barrier Penetration Model) is utilized via the Wong formula as a baseline for comparison.

2.1. Coupled-Channels (CC) Formalism

Coupled-channel calculations are of fundamental importance not only for theoretical investigations but also for obtaining meaningful experimental results. These calculations are applied with high accuracy in energy regimes where coupling effects are most pronounced specifically, below and just above the Coulomb barrier. In this range, the number of coupled channels is limited and computationally manageable; however, at energies well above the barrier, the increasing density of channels complicates the calculations

significantly (Hagino and Takigawa, 2012). In the present study, to maintain modeling simplicity, rearrangement processes (notably transfer reactions) are ignored, and only couplings with inelastic channels are considered.

The total Hamiltonian of the system, describing the relative motion r and the internal degrees of freedom ξ is given by:

$$H(r,\xi) = -\frac{\hbar^2}{2\mu}\nabla^2 + H_{int}(\xi) + V_{rel}(r) + V_{coup}(r,\xi) \quad \textbf{(1)}$$

where μ is the reduced mass, $V_{\mathrm{rel}}(r)$ is the bare potential (the sum of nuclear and Coulomb terms), $H_{\mathrm{int}}(\xi)$ represents the internal Hamiltonians of the target and projectile, and $V_{coup}(r,\xi)$ is the coupling term.

By expanding the total wave function over the internal eigenstates $\phi_n(\xi)$, the coupled Schrödinger equation is obtained as (Thompson and Nunes, 2009):

$$\left(-\frac{\hbar^2}{2\mu}\nabla^2 + \frac{l(l+1)\hbar^2}{2\mu r^2} + V_{rel}(r) + (E - \varepsilon_n)\right)\varphi_n(r) = -\sum_m \langle\phi_n|V_{coup}|\phi_m\rangle\,\varphi_m(r) \quad \textbf{(2)}$$

Incoming Wave Boundary Condition (IWBC): To accurately examine coupling effects on barrier penetration, an alternative boundary condition is preferred over virtual (complex) potentials, as the latter can suppress coupling effects during the tunneling process (Diaz-Torres and Thompson, 2002). The Incoming Wave Boundary Condition (IWBC), as proposed by Rawitscher (1974), addresses this by ensuring that only inward-directed waves exist at a certain radius R_{int} inside the Coulomb barrier:

$$\varphi_n(r) \propto \sqrt{\frac{k_b(r)R_{int}}{k_b(r)}}\,exp\left[-i\int_{R_b}^{r} k_b(r')dr'\right] \quad \textbf{(3)}$$

where $k_b$is the local wave number. The fusion cross-section is then derived from the net incoming flux at R_{int} (Rawitscher, 1974; Diaz-Torres and Thompson, 2002):

$$\sigma_f = \frac{\pi}{k^2}\sum_l (2l+1)P_l(E) \quad \textbf{(4)}$$

2.2. The 1D-BPM Approximation: The Wong Formula

Within the framework developed by Wong (1973), the partial wave cross-section is expressed through a tunneling probability based on the Hill-Wheeler (1953) approximation, which treats the potential barrier as an inverse parabola.

It is crucial to clarify that the Wong formula is a 1D-BPM approximation and not a coupled-channel code. It assumes that barrier properties (height V_b, position R_b, and curvature $\hbar\omega$) are constant for all partial waves. Under these assumptions, the total fusion cross-section is given by (Wong, 1973):

$$\sigma_{fus} = \frac{R_b^2\hbar\omega}{2E}\,ln\left[1 + exp\frac{2\pi}{\hbar\omega}(E - V_b\right] \quad \textbf{(5)}$$

For energies well above the barrier ($E \gg V_{\mathrm{b}}$), this simplifies to the well-known classical expression (Santhosh and Jose, 2014):

$$\sigma_{fus} = \pi R_{\mathrm{b}}^2\left[1 - \frac{V_{\mathrm{b}}}{E}\right] \quad \textbf{(6)}$$

In this study, the Wong formula is used strictly as a non-coupled baseline to highlight the enhancement effects captured by the CCFULL, CCFUS, and NRV codes.

3. Results and Discussions

This study provides a systematic comparative analysis of the CCFULL, CCDEF, CCFUS, and NRV coupled-channel frameworks, alongside the Wong formalism, regarding their efficacy in calculating fusion cross-sections and barrier distributions. By investigating a diverse set of reaction systems, it's aimed to evaluate the consistency of these computational models and establish a robust theoretical baseline. Furthermore, calculations involving stable nuclear systems were performed to provide predictive reference data for reaction channels where experimental measurements are currently lacking.

The heavy-ion fusion cross-sections and their corresponding barrier distributions (D_{fus}) are analyzed in detail and presented through comprehensive graphical representations. The nuclear potential depths (V_0) (URL-1) and surface diffuseness parameters (a_0) (URL-1) utilized in these calculations are summarized in Table 1. The structural properties of the colliding nuclei, including the excitation energies and octupole deformation parameters (β_3), were retrieved from established literature (Spear, 1989) and are detailed in Table 2.

Table 1. Potential parameters used in the coupled-channel calculations for the studied reaction systems. V_0 represents the depth of the real part of the nuclear potential, and a_0 denotes the surface diffuseness parameter.

Reaction	V_0(MeV)	a_0(fm)
^{30}Si+^{26}Mg	53.184	0.633
^{32}S+^{58}Ni	64.095	0.658
^{46}Ti+^{124}Sn	78.702	0.681
^{48}Ti+^{124}Sn	78.380	0.683
^{50}Ti+^{124}Sn	78.095	0.683
^{58}Ni+^{58}Ni	72.816	0.671
^{58}Ni+^{64}Ni	73.873	0.673
^{64}Ni+^{64}Ni	105.100	0.750
^{64}Zn+^{64}Zn	75.447	0.676
^{64}Zn+^{70}Zn	75.447	0.676
^{70}Zn+^{70}Zn	75.920	0.680

Literature review indicates that the ^{30}Si+^{26}Mg reaction was previously investigated both experimentally and theoretically using the CCFULL code by Morsad et al. (1990). In their analysis, the interaction potential was modeled as the sum of the Coulomb potential for two point charges and a real nuclear potential employing the Woods-Saxon form. These calculations show that while most codes converge in the above-barrier region and demonstrate strong agreement with experimental data, the CCFUS code exhibits a noticeable deviation (Figure 1a). This discrepancy arises primarily because the CCFUS model utilizes a simplified coupling scheme that often neglects the specific excitation energies of high-spin states or relies on a constant coupling approximation (the 'abrupt' approximation), which limits its precision in systems with complex channel couplings.

The observed discrepancy in the CCFUS results for the ^{30}Si+^{26}Mg system can be attributed to the simplified treatment of excitation energies and the constant coupling approximation inherent in the code's algorithm. Unlike CCFULL or NRV, which perform a more rigorous radial integration of the coupled equations, CCFUS employs a simplified 'constant-coupling' approximation where the coupling matrix elements are evaluated at the barrier radius (R_{b}). In systems where the excitation energies are relatively high or the potential surface is significantly deformed, this approximation fails to capture the energy-dependence of the tunneling process. For the ^{30}Si+^{26}Mg case, the coupling to the 2^+ states in both nuclei introduces a redistribution of the barrier that CCFUS cannot fully resolve, leading to the observed underestimation of the fusion cross-section below the barrier.

The corresponding fusion barrier distributions are presented in Figure 1b. Both CCFULL and NRV explicitly account for channel coupling effects, resolving the inherent structure of the barrier. In contrast, while the Wong formalism can approximate the average position and width of the experimental distribution, it remains a single-barrier approximation that cannot resolve the multi-peaked structure resulting from collective excitations. Nevertheless, the peak positions of the calculated distributions show reasonable consistency across the different frameworks, validating the chosen potential parameters.

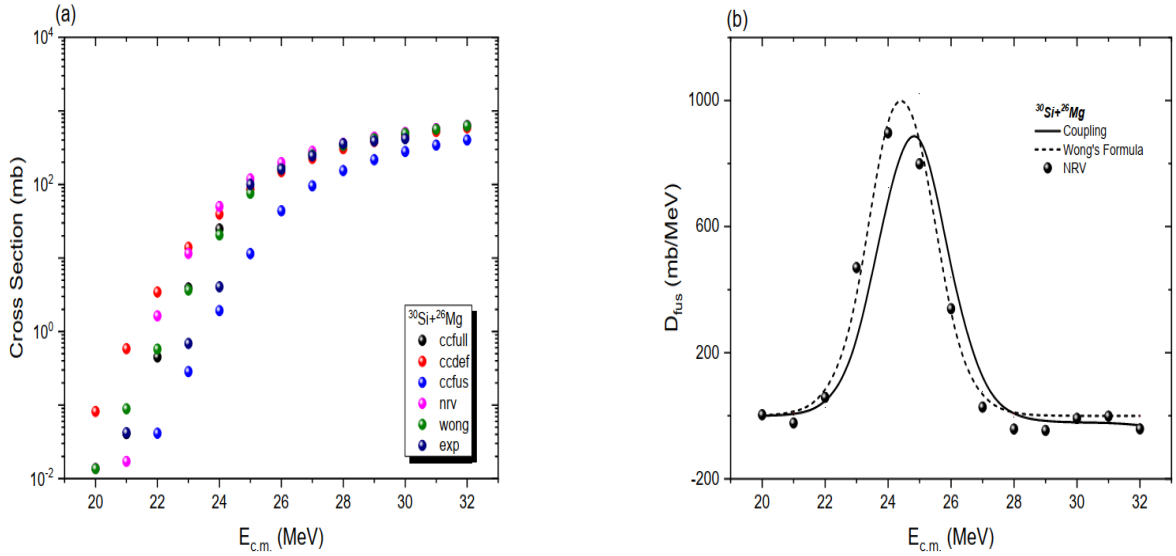

Figure 1. (a) Fusion excitation functions and (b) corresponding D_{fus} for the ^{30}Si+^{26}Mg system. Calculations from CCFULL and NRV are compared with experimental data. The Wong formula is included in panel (a) as a 1D-BPM baseline, while panel (b) highlights the multi-peaked structure arising from channel couplings.

^{32}S+^{58}Ni reaction was analyzed within the center-of-mass energy range of 60–90 MeV using various coupled-channel frameworks and the Wong formalism (Figure 2a). The calculated fusion cross-sections were benchmarked against the experimental data reported by Stefanini et al. (1987). For this system, the potential depth was set to 64.09 MeV, corresponding to a nominal Coulomb barrier of 60.21 MeV. As illustrated in the excitation function, all computational models demonstrate high consistency, accurately reproducing the experimental data both at the barrier and in the above-barrier regions.

The fusion barrier distributions are presented in Figure 2b. Given the Coulomb barrier value of 60.21 MeV, the energy intervals for the cross-section and barrier distribution analyses were optimized to capture the relevant tunneling dynamics. In this region, the results from CCFULL, NRV, and the Wong formula converge to a prominent peak near the barrier energy. While the Wong model yields a symmetric, smooth distribution characteristic of its parabolic approximation, the coupled-channel results reflect the underlying collective excitations, providing a more robust physical representation of the barrier structure compared to a standard Gaussian approximation.

The fusion excitation functions for the ^{46,48,50}Ti+^{124}Sn isotopic series are presented as a function of center-of-mass energy in Figures 3a, 4a, and 5a, respectively. These coupled-channel calculations are benchmarked against the experimental data and theoretical CCFULL results reported by Liang et al. (2016). At sub-barrier energies, the CCFULL and CCDEF models demonstrate strong agreement with the experimental measurements, effectively capturing the fusion enhancement. In the above-barrier region, all computational frameworks, including the simplified models, converge and align well with the experimental trends.

To further elucidate the underlying reaction mechanisms and the role of internal degrees of freedom, the fusion barrier distributions were extracted. Theoretically, these distributions are related to the second derivative of the product of the cross-section and energy. As shown in Figures 3b, 4b, and 5b, the distributions obtained from NRV and CCFULL are highly consistent, occupying the same energy axis and reproducing the structured barrier profiles. A comparative

analysis reveals that the Wong formalism tends to produce a single, slightly narrower peak with a higher magnitude than the CC results. The systematic evolution of these distributions across the Ti isotopes illustrates the sensitivity of the fusion process to the increasing neutron number and the corresponding collective vibrational modes of the target and projectile.

As seen in Figures 3-5, the increasing neutron number in the Ti isotopes leads to a subtle broadening of the barrier distribution, a feature captured with varying degrees of precision by the CCFULL and NRV codes, while remaining outside the scope of the 1D-BPM Wong model.

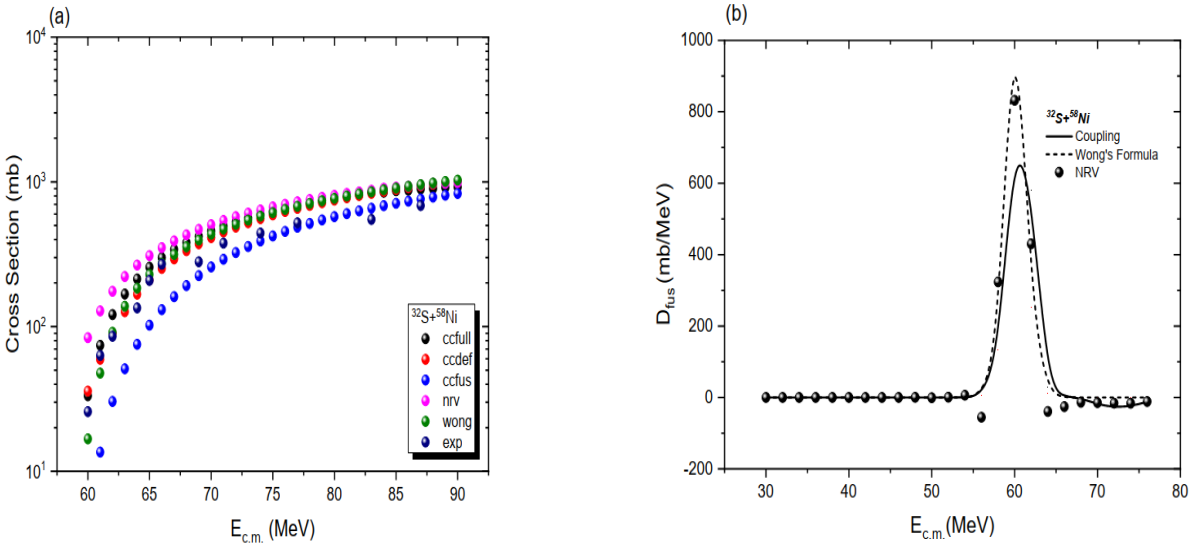

Figure 2. (a) Fusion excitation functions and (b) corresponding D_{fus} for the ^{32}S+^{58}Ni system. The CCFULL and NRV calculations are compared against experimental data. The Wong formula is included in panel (a) as a 1D-BPM reference, while the distribution in panel (b) demonstrates the impact of collective excitations on the barrier structure.

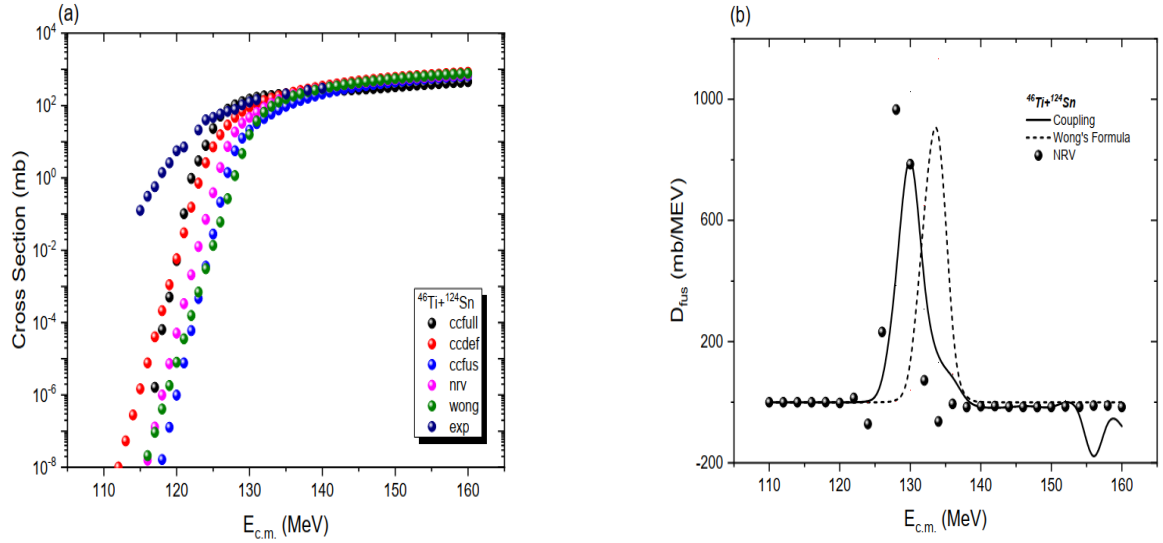

Figure 3. (a) Fusion excitation functions and (b) D_{fus} for the ^{46}Ti+^{124}Sn reaction. The CCFULL and NRV calculations are presented alongside experimental data. The Wong formula is included in (a) to illustrate the 1D-BPM baseline. The structured barrier distribution in (b) highlights the strong influence of the target's collective vibrational states on the fusion process at sub-barrier energies.

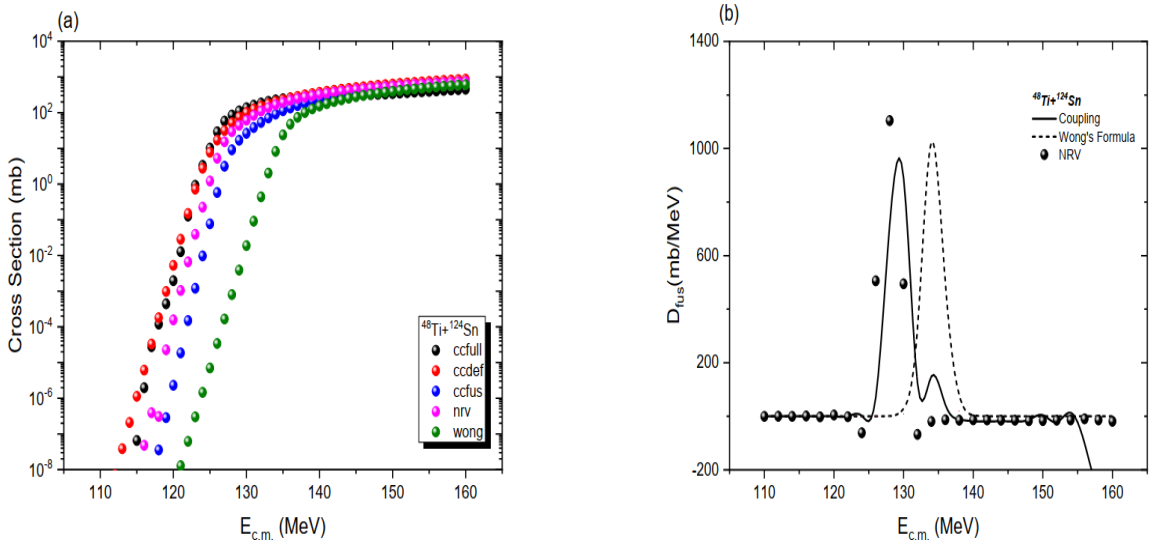

Figure 4. (a) Fusion excitation functions and (b) corresponding D_{fus} for the ^{48}Ti+^{124}Sn system. Calculations from CCFULL and NRV are compared with experimental data, while the Wong formula is shown in panel (a) as a 1D-BPM reference. The barrier distribution in (b) reflects the shift in fusion dynamics due to the increased neutron number in the projectile, illustrating the sensitivity of the D_{fus} structure to isotopic variations.

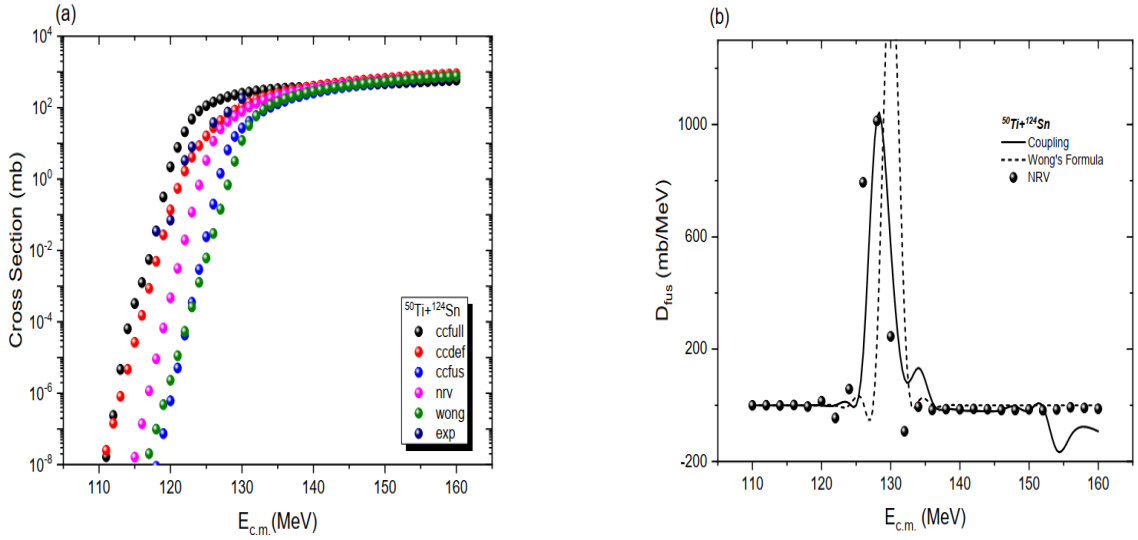

Figure 5. (a) Fusion excitation functions and (b) D_{fus} for the ^{50}Ti+^{124}Sn system. The experimental data are compared with CCFULL and NRV calculations. The Wong formula is included in (a) as a 1D-BPM baseline. The results in (b) demonstrate how the coupled-channel models resolve the barrier structure for this increasingly neutron-rich system, providing a more rigorous treatment of the interaction than the simplified Wong approximation.

Table 2. Experimental excitation energies (E_x) and octupole deformation parameters (β_3) for the 3^- states of the target nuclei (Raman et al. (1989), Spear (1989), URL-1). These values were used as input parameters for the coupled-channel calculations to account for collective vibrational excitations.

Target	E_x (MeV)	β_3
^{26}Mg	6.876	0.213
^{58}Ni	4.475	0.198
^{64}Ni	3.560	0.201
^{124}Sn	2.603	0.106
^{64}Zn	2.998	0.233
^{70}Zn	2.859	0.210

The fusion barrier distributions for the Ni+Ni systems are illustrated in Figures 6b and 7b, where theoretical results are benchmarked against the experimental data of Beckerman et al. (1982). A detailed examination of the NRV results reveals a distribution that is slightly broader than those produced by the other frameworks. This behavior suggests that the representation of the barrier structure in NRV is highly sensitive to the number of coupled channels included in the calculation. Specifically, for the ^{58}Ni+^{64}Ni system, increasing the channel coupling beyond the fundamental vibrational states may be required to achieve a more refined convergence and further resolve the distribution profile.

Despite these subtle variations in width, the peak positions obtained from NRV, CCFULL, and the Wong formula remain consistent with one another. This agreement indicates that while the fine structure of the distribution depends on the complexity of the coupling scheme, the average barrier height is reliably captured across all three methods. Consequently, the calculations remain physically grounded and provide a consistent basis for interpreting the fusion dynamics of these nickel-based reactions.

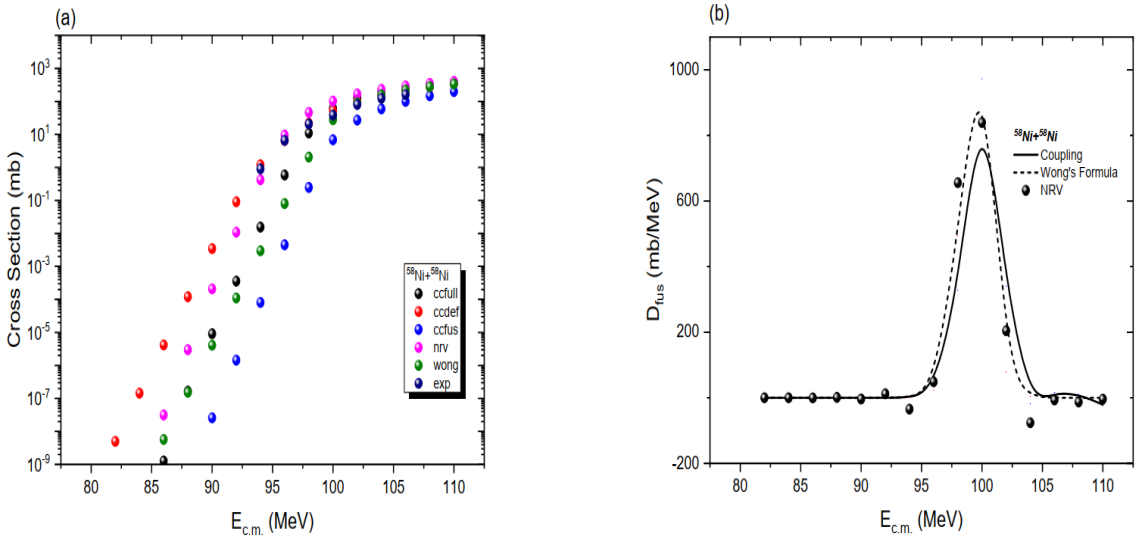

Figure 6. (a) Fusion excitation functions and (b) corresponding D_{fus} for the ^{58}Ni+^{58}Ni reaction. Calculations from CCFULL and NRV are compared with experimental data. The Wong formula is included in (a) as a 1D-BPM baseline. For this symmetric system, the structured distribution in (b) illustrates the strong sub-barrier enhancement effect arising from multi-phonon vibrational couplings, which is captured with high precision by the coupled-channel codes.

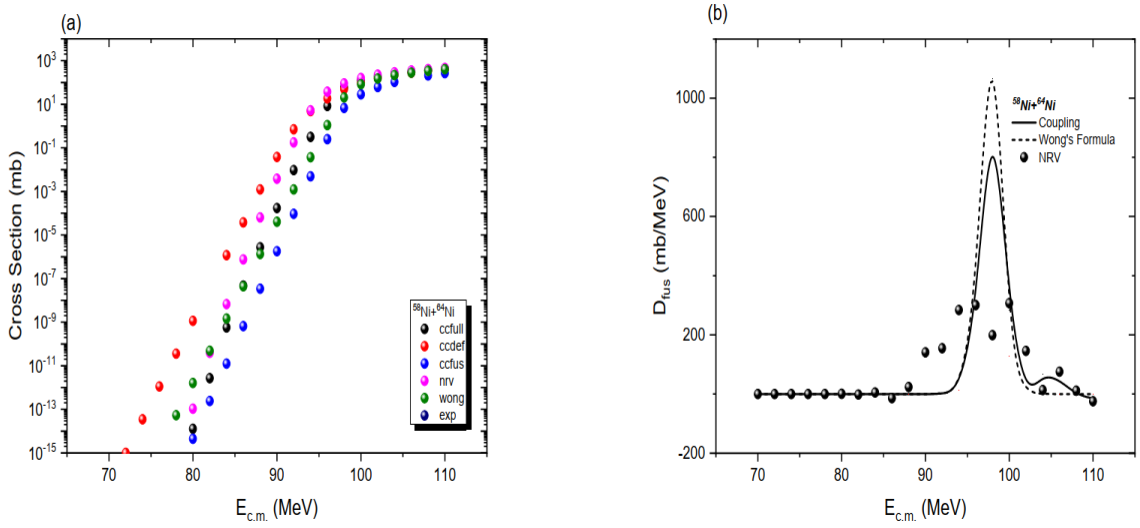

Figure 7. (a) Fusion excitation functions and (b) D_{fus} for the asymmetric ^{58}Ni+^{64}Ni system. The CCFULL and NRV calculations are compared with experimental data, using the Wong formula in panel (a) as a 1D-BPM reference. The observed broadening in the barrier distribution in (b) highlights the increased complexity of the coupling scheme in this system, where the interplay between collective excitations and potential transfer channels significantly influences the sub-barrier fusion enhancement.

The reaction series comprising ^{64}Zn+^{64}Zn, ^{64}Zn+^{70}Zn, and ^{70}Zn+^{70}Zn provides a systematic framework to investigate the impact of isospin asymmetry on fusion dynamics. In these systems, the atomic number (Z) remains constant, thereby eliminating Coulombic variations, while the varying mass number (A) introduces neutrality-related structural changes. A primary motivation for analyzing this series is the current lack of experimental fusion cross-section data in the literature; thus, the theoretical results obtained in this study are established as a predictive benchmark for future experimental efforts.

The nominal Coulomb barriers (V_{B}) for these reactions were determined to be 108.12 MeV, 109.85 MeV, and 111.41 MeV, respectively. As illustrated in the excitation functions (Figures 8a, 9a, and 10a), all computational models demonstrate high convergence near and above the barrier region. Correspondingly, the barrier distribution functions, shown in Figures 8b, 9b, and 10b, reveal a strong agreement between the CCFULL and NRV frameworks, both of which explicitly incorporate channel coupling effects. While the Wong formalism yields a peak consistent with the average barrier energy, the coupled-channel results exhibit a subtle shift. Specifically, the inclusion of finite excitation energies within the CCFULL code leads to a slight reduction in the average fusion barrier a phenomenon that can be attributed to the nuclear polarization effect, where the intrinsic degrees of freedom effectively lower the potential energy surface during the approach.

In the ^{64}Zn+^{70}Zn case, the slight variations between NRV and CCFULL in the sub-barrier region suggest that the numerical handling of the coupling strength for the ^{70}Zn vibrational states is sensitive to the specific boundary conditions used in each code.

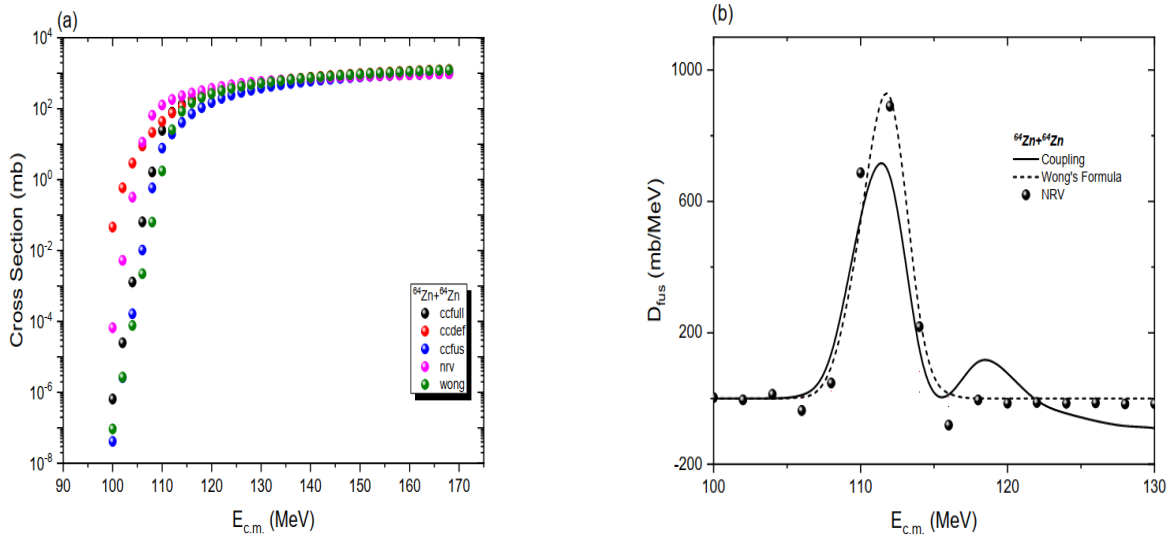

Figure 8. (a) Fusion excitation functions and (b) D_{fus} for the ^{64}Zn+^{64}Zn symmetric system. The CCFULL and NRV calculations are presented alongside experimental data, with the Wong formula included in (a) as a 1-D BPM baseline. The structure of the barrier distribution in (b) underscores the essential role of collective degrees of freedom in enhancing the fusion probability, a feature that the coupled-channel formalism resolves more effectively than the single-barrier approximation.

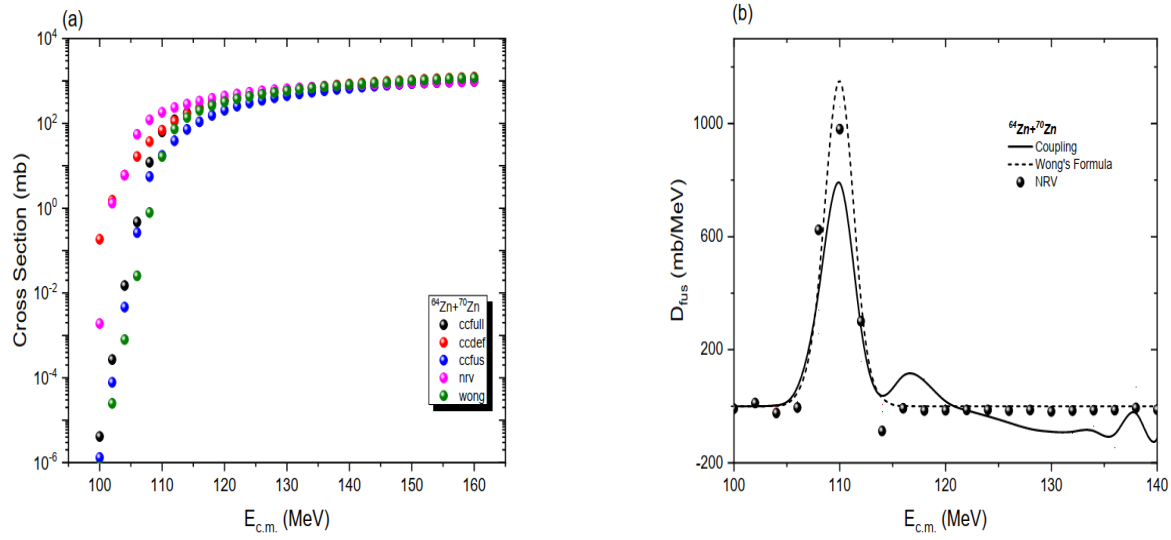

Figure 9. (a) Fusion excitation functions and (b) D_{fus} for the asymmetric ^{64}Zn+^{70}Zn system. The CCFULL and NRV results are compared with experimental data, using the Wong formula in panel (a) as a 1D-BPM baseline. The distribution in (b) reflects the influence of the increased neutron number in the target, where the coupling to collective states leads to a characteristic broadening of the barrier structure that is well-captured by the coupled-channel calculations.

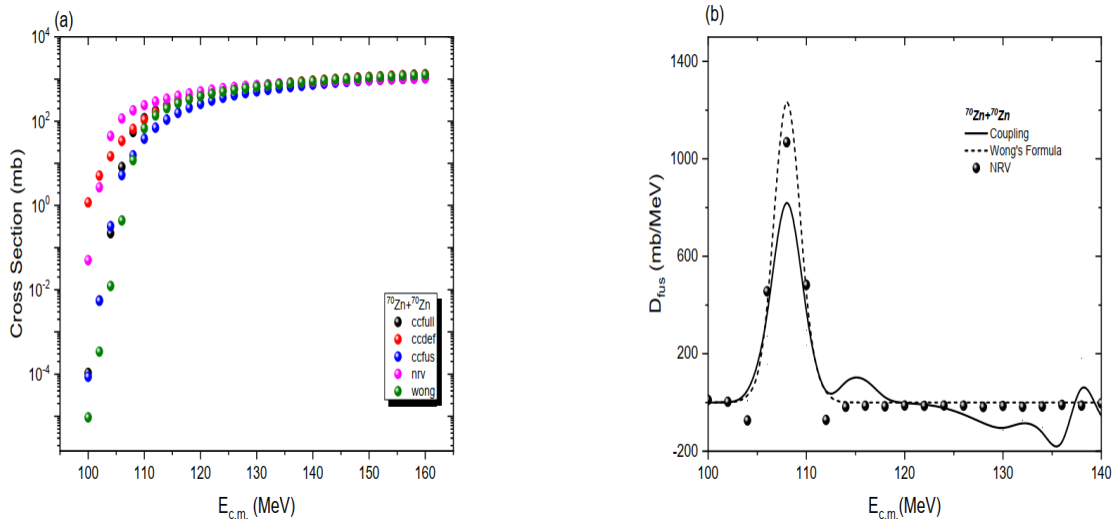

Figure 10. (a) Fusion excitation functions and (b) D_{fus} for the symmetric ^{70}Zn+^{70}Zn reaction. Experimental data are compared with CCFULL and NRV calculations, using the Wong formula in (a) as a 1D-BPM baseline. The structure in (b) illustrates the collective response of this neutron-rich symmetric system, where the coupled-channel codes successfully resolve the redistribution of the fusion barrier, a feature that becomes increasingly prominent with the higher mass number of the isotopes.

4. Conclusion

This comparative analysis of ^{30}Si+ ^{26}Mg, ^{32}S+ ^{58}Ni, ^{46,48,50}Ti+ ^{124}Sn,^{58,64}Ni+ ^{58,64}Ni, ^{64,70}Zn+ ^{64,70}Zn systems highlights the critical role of coupled-channel effects in heavy-ion fusion dynamics. The results demonstrate that while the one-dimensional Barrier Penetration Model, such as the Wong formalism, consistently underestimates sub-barrier fusion cross-sections, a rigorous accounting for internal degrees of freedom specifically collective vibrational excitations 2^+ and 3^- states) is essential for an accurate physical description.

By utilizing identical nuclear potential parameters across CCFULL, NRV, CCDEF, and CCFUS, a consistent benchmark has been ensured. While all codes converge in the above-barrier region, significant structural differences emerge in the barrier distribution, near and below the Coulomb barrier. Notably, CCFULL and NRV, which employ full quantum mechanical coupling schemes, effectively resolve the multi-peaked structure of barrier distribution. This structure reflects the splitting of the single static barrier into a spectrum of barriers, thereby enhancing tunneling probabilities.

The systematic analysis of Ti, Ni, and Zn isotopic chains (Figures 1–10) reveals that fusion enhancement is highly sensitive to deformation parameters (β_2, β_3) and neutron-richness. Specifically, for the ^{58}Ni+ ^{64}Ni system, the number of coupled-channels in the NRV calculations was carefully tested for convergence. While the distribution appears broader than in the symmetric ^{58}Ni+ ^{58}Ni case, further increasing the channel coupling leads to numerical saturation. This confirms that the observed width is a physical reflection of the coupling strength rather than a lack of convergence. As neutron numbers increase, CCFULL and NRV consistently capture these subtle dynamics, whereas the 1D-BPM remains insufficient.

In conclusion, while all tested models are physically consistent for general cross-section estimations, CCFULL and NRV provide superior resolution of the barrier distribution compared to the simplified CCFUS and CCDEF models. This

precision is crucial for future research into superheavy element synthesis and exotic nuclei reactions, where the exact shape of the fusion barrier dictates reaction outcomes. The robust agreement between these advanced simulations and experimental data reinforces the coupled-channel framework as a vital predictive tool for unexplored nuclear reactions.

Author Contributions This work was entirely conducted and prepared by Erol, B. All aspects of conceptualization, data analysis, interpretation, and manuscript writing were carried out solely by the author.

Funding Statement This research did not receive any specific grant from funding agencies, commercial entities, or not-for-profit organizations.

Conflict of Interest Statement: The author declares that there is no conflict of interest.

References

Beckerman, M., Salomaa, M., Sperduto, A., Molitoris, J.D. (1982). Sub barrier fusion of ^{58,64}Ni with ^{64}Ni and ^{74}Ge. *Physical Review C*, 25, 837–849. https://doi.org/10.1103/PhysRevC.25.837

Cheng, K. X., Xu, C., Ma, C. W., Pu, J., Wang, Y.T. (2022). Pauli blocking potential applied to heavy-ion fusion reactions. *Chinese Physics C*, 46, 024105. https://doi.org/10.1088/1674-1137/ac4c1d

Dasso, C.H. (1987). CCFUS – A simplified coupled-channel code for calculation of fusion cross sections in heavy-ion reactions. *Computer Physics Communications*, 46(3), 187–191. https://doi.org/10.1016/0010-4655(87)90105-7

Del Fabbro, M., Stefanini, A.M., Montagnoli, G., Corradi, L., Fioretto, E., Fornalè, M., Szilner, S. (2023). Influence of the Z = 50 shell closure on heavy-ion sub-barrier fusion. *European Physical Journal A*, 59, 26. https://doi.org/10.1140/epja/s10050-023-00026-x

Deng, W., Cheng, K., Xu, C. (2025). Sub-barrier fusion cross sections: Role of Pauli blocking and isospin asymmetry. *Chinese Physics C*, 49, 054109. https://doi.org/10.1088/1674-1137/abf123

Denisov, V.Y. (2023). Expression for the heavy-ion fusion cross section. *Physical Review C*, 107, 054618. https://doi.org/10.1103/PhysRevC.107.054618

Denisov, V.Y., Jin, Y. (2022). Heavy-ion fusion cross section formula and barrier height distribution. *Physical Review C, 105*, 064601. https://doi.org/10.1103/PhysRevC.105.064601

Diaz-Torres, A., Thompson, I.J. (2002). Coupled-channels calculations in fusion reactions with weakly bound nuclei. *Physical Review C*, 65(2), 024606. https://doi.org/10.1103/PhysRevC.65.024606

Erol, B., Cinan, Z.M., Başkan, T., Yılmaz, A.H. (2021). Investigating medium and heavy mass heavy ion fusion reactions and barrier distributions with coupled channel analyses. *Acta Physica Polonica B*, 52(9), 1117–1145. https://doi.org/10.5506/aphyspolb.52.1117

Fernández Niello, J., Dasso, C.H., Landowne, S. (1989). CCDEF – A simplified coupled channel code for fusion cross sections including static nuclear deformations. *Computer Physics Communications*, 54(1–2), 409–417. https://doi.org/10.1016/0010-4655(89)90100-8

Gharaei, R., Fuji, A., Azadegan, B. (2021). Survey of deep sub-barrier heavy-ion fusion hindrance phenomenon for positive and negative Q-value systems using the proximity-type potential. *Chinese Physics C*, 45(12), 124101. https://doi.org/10.1088/1674-1137/ac23d3

Hagino, K., Rowley, N., Kruppa, A.T. (1999). A program for coupled channel calculations with all order couplings for heavy ion fusion reactions. *Computer Physics Communications*, 123(2–3), 143–152. https://doi.org/10.1016/S0010-4655(99)00134-2

Hagino, K., Takigawa, N. (2012). Subbarrier fusion reactions and many-particle quantum tunneling. *Progress in Particle and Nuclear Physics*, 66(1), 1–86. https://doi.org/10.1016/j.ppnp.2010.11.002

Hill, D.L., Wheeler, J.A. (1953). Nuclear constitution and the interpretation of fission phenomena. *Physical Review*, 89(5), 1102–1145. https://doi.org/10.1103/PhysRev.89.1102

Jiang, C.L., Henning, W.F., Kay, B.P., Watwood, N. (2023). Structures in the heavy-ion fusion excitation function at and above the Coulomb barrier. *Physical Review C*, 108, L051604. https://doi.org/10.1103/PhysRevC.108.L051604

Liang, J.F., Allmond, J.M., Gross, C.J., Mueller, P. E., Shapira, D., Varner, R.L. (2016). Examining the role of transfer coupling in sub barrier fusion of ^{46,50}Ti + ^{124}Sn. *Physical Review C*, 94(2), 024616. https://doi.org/10.1103/PhysRevC.94.024616

Montagnoli, G., Stefanini, A.M. (2023). Recent experimental results in sub- and near-barrier heavy-ion fusion reactions (2nd ed.). *European Physical Journal A*, *59*, 138. https://doi.org/10.1140/epja/s10050-023-01001-0

Morsad, A., Kolata, J.J., Tighe, R.J., Kong, X.J., Aguilera, E.F., Vega, J.J. (1990). Subbarrier fusion of ^{28,30}Si with ^{24,26}Mg. *Physical Review C*, 41(3), 988–994. https://doi.org/10.1103/PhysRevC.41.988

Raman, S., Nestor, C.W., Jr., Kahane, S., Bhatt, K.H. (1989). Predictions of $B(E2; 0_1^+ \rightarrow 2_1^+)$ values for even-even nuclei. *Atomic Data and Nuclear Data Tables*, 42(1), 1–54. https://doi.org/10.1016/0092-640X(89)90031-4

Rawitscher, G.H. (1974). Fusion reactions with a realistic optical potential and the incoming-wave boundary condition. *Physical Review C*, 9(6), 2210–2217. https://doi.org/10.1103/PhysRevC.9.2210

Santhosh, K.P., Jose, V.B. (2014). Heavy-ion fusion cross sections of weakly bound ^{9}Be on ^{27}Al, ^{64}Zn and tightly bound ^{16}O on ^{64Zn} target using Coulomb and proximity potentials. *Nuclear Physics A*, *922*, 191–199.

Singh, V., Lahiri, J., Roy Chowdhury, P., Basu, D.N. (2021). Hindrance in heavy-ion fusion for lighter systems of astrophysical interest. *arXiv preprint* arXiv:2107.09451. https://arxiv.org/abs/2107.09451

Spear, R.H. (1989). Reduced electric-octupole transition probabilities, $B(E3;0_1^+ \rightarrow 3_1^-)$, for even-even nuclides throughout the periodic table. *Atomic Data and Nuclear Data Tables*, 42(1), 55–104. https://doi.org/10.1016/0092-640X(89)90032-6

Stefanini, A.M., Bonamini, D., Tivelli, A., Montagnoli, G., Fortuna, G., Nagashima, Y., Beghini, S., Signorini, C., DeRosa, A., Inglima, G., Sandoli, M., Cardella, G., Rizzo, F. (1987). Strong energy dependence of the optical potential for ^{32}S + ^{58},64Ni near the Coulomb barrier. *Physical Review Letters*, 59(12), 2852–2855. https://doi.org/10.1103/PhysRevLett.59.2852

Thompson, I.J., Nunes, F.M. (2009). *Nuclear reactions for astrophysics: Principles, calculation and applications of low-energy reactions*. Cambridge University Press.

URL–1, (2020). NRV Web Knowledge Base. Joint Institute for Nuclear Research – Low energy nuclear physics. http://nrv.jinr.ru/nrv/, 02.01.2020.

Vijay, N., Grover, N., Sharma, K., Gautam, M.S., Sharma, M.K., Chahal, R.P. (2022). Fusion fission analysis of ^{12}C + ^{248}Cm and ^{16}O + ^{244}Pu nuclear reactions across the Coulomb barrier. *Physical Review C*, 106, 064609. https://doi.org/10.1103/PhysRevC.106.064609

Wong, C.Y. (1973). Interaction barrier in charged-particle nuclear reactions. *Physical Review Letters*, 31(12), 766–769. https://doi.org/10.1103/PhysRevLett.31.766